

*Letter to the Editor***Spectroscopic study of high redshift quasars***

M. Dietrich¹, I. Appenzeller^{1,4}, S.J. Wagner¹, W. Gässler³, R. Häfner³, H.-J. Hess³, W. Hummel³, B. Muschielok³, H. Nicklas², G. Rupprecht⁵, W. Seifert¹, O. Stahl¹, T. Szeifert^{5,1}, and K. Tarantik³

¹ Landessternwarte Heidelberg, Königstuhl, 69117 Heidelberg, Germany

² Universitätssternwarte Göttingen, Geismarlandstrasse 11, 37083 Göttingen, Germany

³ Universitätssternwarte München, Scheinerstrasse 1, 81679 München, Germany

⁴ Max-Planck-Institut für Astronomie, Königstuhl, 69117 Heidelberg, Germany

⁵ ESO Garching, Germany

Received 9 August 1999 / Accepted 23 August 1999

Abstract. We obtained optical spectra of four quasars with $3 < z < 4$ and SDSSp J033829.31+002156.3 with $z = 5.0$ with FORS 1 at the VLT UT1 Antu. To estimate the relative abundances of the line emitting gas we used the line ratios NV1240/CIV1549, NV1240/HeII1640, and OVI1034/HeII1640 as suggested by Hamann & Ferland (1992, 1999). Based on chemical evolutionary models we estimate a metallicity of $Z \simeq 7 Z_{\odot}$ for the quasars with $z \simeq 3$ within the framework of the rapid star formation scenario. Even Q0338+0021 indicates a comparable high relative abundance. Our results provide support for supersolar metallicities at very high redshifts of $z \simeq 5$.

Key words: cosmology: early Universe – galaxies: quasars: emission lines

1. Introduction

Spectroscopic studies of quasars at high redshift ($z \geq 3$) indicate metallicities of the emission line gas enhanced by up to one order of magnitude compared to solar values (cf. Hamann & Ferland 1992; Osmer et al. 1994; Ferland et al. 1996; Hamann & Ferland 1999). These high metallicities must have been caused by early violent star formation events. As shown by the authors mentioned above, comparisons of quasar emission line fluxes with chemical evolution models provide a powerful tool to constrain the formation and evolution of massive stars in the early universe. Particularly informative are the abundance ratios of α -elements (such as C, O, Mg) and secondary elements (such as N) (see e.g. Hamann & Ferland 1993; Korista et al. 1996; Pettini 1999). A summary of this work can be found in a recent review by Hamann & Ferland (1999). However, most of these results

Table 1. coordinates, apparent brightness, and redshift of the observed quasars. The apparent brightness was taken from Véron-Cetty & Véron (1991) with the exception of SDSSp J033829.31+002156.3, quoted Q0338+0021 in the following. The given brightness $m_{r'}$ for this quasar is provided by Fan et al. (1999).

object	$\alpha_{2000.0}$	$\delta_{2000.0}$	m_v	z
Q0044-273	00 47 10.8	−27 04 41	20.3	3.16
Q0046-282	00 49 24.4	−27 59 02	19.7	3.83
Q0103-294	01 06 02.8	−29 08 59	20.2	3.11
Q0103-260	01 06 04.3	−25 46 53	18.8	3.36
Q0338+0021	03 38 29.3	+00 21 56	21.7	5.00

have been based on quasars with redshifts below $z \simeq 3$ and only relatively little data exist for higher redshifted QSOs. Therefore, we measured new emission line flux values for 5 quasars with redshifts between 3.1 and 5.0 which had been observed (for instrumental test purposes) during the commissioning phase of the FORS 1 instrument at the ESO VLT.

2. Observations

All observations were carried out with FORS 1 at the VLT unit telescope Antu in September, October, and December 1998 using the long-slit spectroscopic mode. Since the objective of the observations was to check and derive instrumental functions and parameters, very different observational conditions and relatively short exposure times were used. Some of the spectra were obtained during bright moonlight. The spectra of Q0044-273 were taken close to the full moon, resulting in a rather low S/N in the blue spectral range (cf. Figs. 1,2). Table 1 lists the coordinates, redshifts, and apparent brightness of the observed quasars.

The observing dates, grisms (cf. FORS users guide, <http://www.eso.org/instruments/fors1/>), integration times, and slit widths are listed in Table 2. The wavelength calibration was carried out using HeHgCd lamps. The spectral resolutions

Send offprint requests to: M. Dietrich
(mdietric@lsw.uni-heidelberg.de)

* Based on observations with the VLT-UT1 operated on Cerro Paranal (Chile) by the European Southern Observatory

Table 2. obs.log of the high-redshift quasars which were observed with FORS 1

object	date	UT _{start}	t _{int} [sec]	grism	slit width
Q0044-273	Oct., 04	06 41 23	900	150I	1''0
	Oct., 04	06 59 39	1800	600B	1''0
Q0046-282	Sep., 22	08 43 40	600	150I	0''7
	Sep., 22	08 56 28	600	150I	0''7
Q0103-294	Sep., 25	02 59 48	900	150I	0''7
	Sep., 25	03 17 31	900	150I	0''7
	Sep., 25	03 37 32	1200	600B	0''7
Q0103-260	Sep., 24	07 14 21	900	150I	1''0
	Sep., 24	07 33 18	900	150I	1''0
	Sep., 24	07 47 53	1800	600B	1''0
	Dec., 16	04 05 24	1800	600B	0''4
	Dec., 19	04 00 59	1800	600B	0''4
	Dec., 26	01 53 02	1800	600B	0''4
Q0338+0021	Dec. 26	03 11 16	1800	300I	1''0
	Dec. 26	03 43 12	1800	300I	1''0

$\lambda/\Delta\lambda$ ranged between about 400 (Grism 150I, 1''0 slit), and about 2000 (Grism 600B, 0''4 slit). For flux calibrations the standard star LTT 9491 was observed with the same grisms. For the atmospheric extinction correction we used - in the absence of suitable mean data for Paranal - the standard extinction curve of La Silla (Schwarz & Melnick 1993).

For the four $3 < z < 4$ quasars no removal of the atmospheric absorption features was attempted. Therefore, the strong atmospheric A and B bands (at $\approx 7600 \text{ \AA}$ and $\approx 6900 \text{ \AA}$) and are clearly visible (Fig. 1). In some cases the outer wings of the broad emission lines are affected by telluric absorptions. However, this had little influence on our measurements. In the case of Q0338+0021 we used a standard star spectrum to remove the atmospheric absorption features. The strong atmospheric absorption between 9300 \AA and 9800 \AA (affecting the red wing of the CIV resonance line) was apparently not fully corrected (Fig. 3). The redshifted HeII 1640 line is just beyond this region of strong atmospheric absorption, but its S/N is low, as this line falls close to the CCD's red sensitivity cutoff.

Since all objects have high galactic latitudes, no corrections for interstellar extinction were applied.

The 2D longslit spectra were reduced and analysed using standard MIDAS software. Individual spectra taken with the same settings were averaged to improve the signal-to-noise ratio. The resulting mean quasar spectra in the wavelength ranges of the three grisms are displayed in Figs. 1 to 3. Line flux values were measured by integrating over the line profiles. Since most of the emission lines in our spectra are blended, we first deconvolved the blends assuming similar line profiles for all high ionization metal lines. As template line profile we used the apparently least blended strong line of CIV1549. In Q0338-0021 we used SiIV/OIV1402 as a template (and for deriving the redshift) since the red wing of C IV is affected by (atmospheric?) absorption.

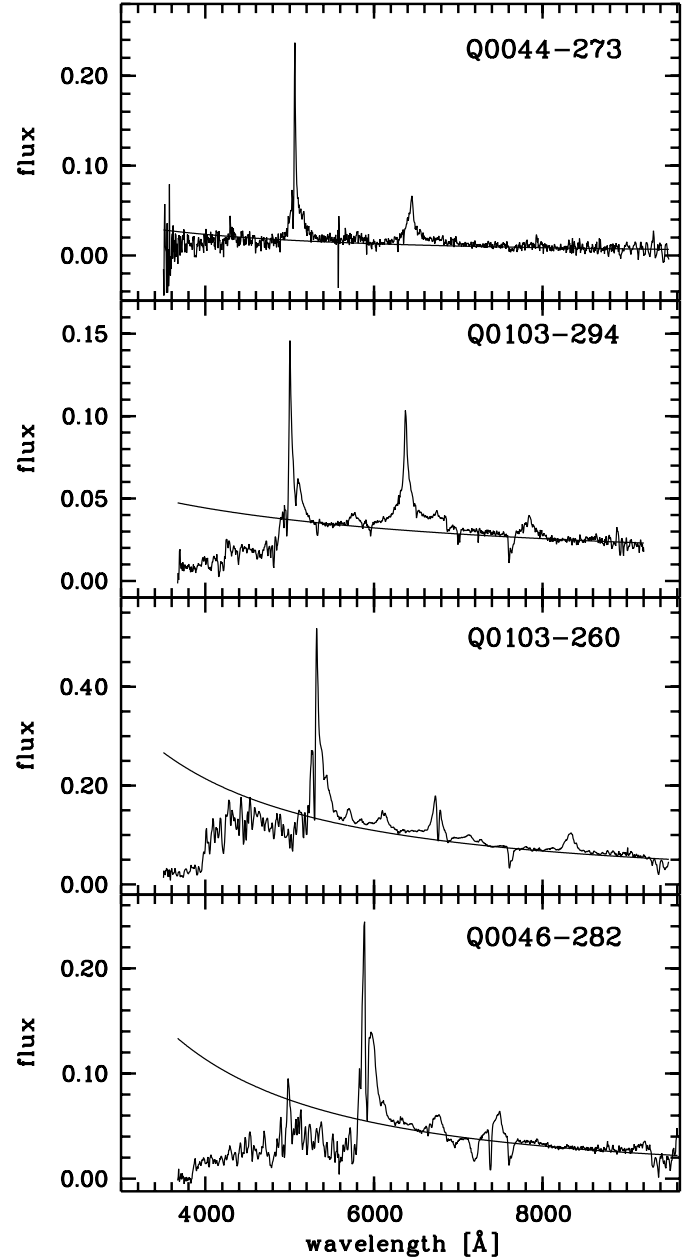


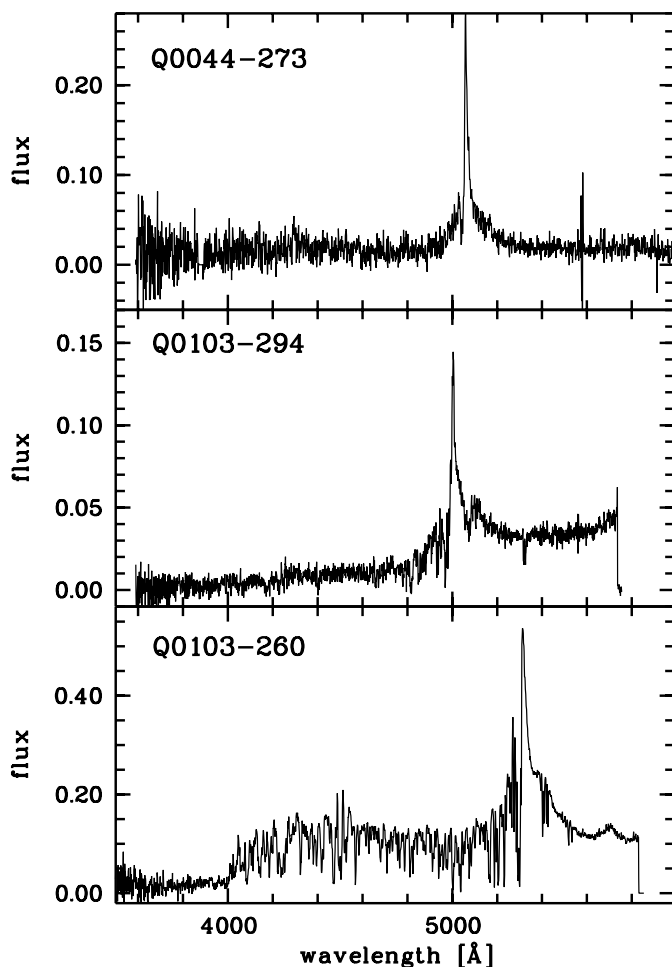
Fig. 1. The spectra of the $3 < z < 4$ quasars which were taken with grism 150I. The flux is given in units of $[10^{-15} \text{ erg s}^{-1} \text{ cm}^{-2} \text{ \AA}^{-1}]$. In each case a power law continuum fit has been included. The corresponding spectral index α , $F_\nu \sim \nu^{-\alpha}$, is listed in Table 3.

3. Results and discussion

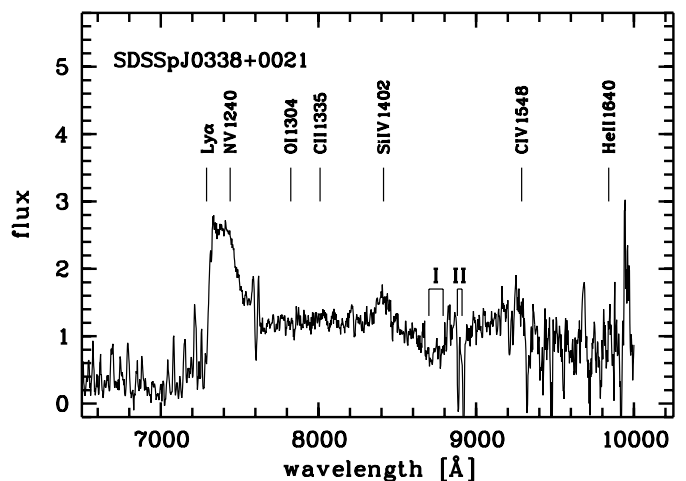
The observed emission line fluxes are listed in Table 3. Also given in Table 3 are the observed NV/CIV, NV/HeII, OIV/CIV and Ly α /CIV flux ratios, which are used to estimate metallicities and the enrichment history of the emission line gas (see e.g. Hamann & Ferland 1999). Particularly important are the ratios involving the α elements synthesized in SN Type II explosions of short-lived massive stars vs. the more slowly evolving secondary element abundances such as nitrogen. We used the emission line ratios of NV1240/CIV1549, NV1240/HeIII1640,

Table 3. The measured emission-line flux of the quasars

line	$F_{\text{obs}} [10^{-15} \text{ erg s}^{-1} \text{ cm}^{-2}]$				
	Q0044-273	Q0046-282	Q0103-294	Q0103-260	Q0338+0021
OVI 1034	1.14 ± 0.20	2.27 ± 0.21	–	8.3 ± 2.00	–
Ly α 1215	10.40 ± 0.50	19.90 ± 1.00	12.00 ± 1.00	38.9 ± 1.20	5.00 ± 1.00
NV 1240	3.35 ± 0.50	7.60 ± 1.00	3.80 ± 0.40	8.33 ± 0.70	1.61 ± 0.16
OI 1304	0.34 ± 0.08	0.70 ± 0.10	–	3.6 ± 0.20	0.13 ± 0.04
CII 1335	–	0.80 ± 0.10	–	1.8 ± 0.30	0.24 ± 0.06
SiIV 1402	1.32 ± 0.10	2.88 ± 0.15	1.44 ± 0.30	6.1 ± 0.30	0.67 ± 0.05
CIV 1548	8.10 ± 0.30	4.89 ± 0.10	10.64 ± 0.30	14.6 ± 0.90	1.70 ± 0.34
HeII 1640	1.65 ± 0.40	0.73 ± 0.15	1.13 ± 0.20	2.06 ± 0.30	0.30 ± 0.15
OIII] 1663	0.29 ± 0.06	–	0.80 ± 0.20	1.10 ± 0.30	–
NIII] 1750	–	–	0.38:	–	–
FeII UV191	–	–	0.21:	0.84 ± 0.20	–
AlIII 1859	–	–	–	1.23 ± 0.30	–
CIII] 1909	0.99 ± 0.06	1.63:	2.88 ± 0.40	6.6 ± 0.40	–
α	0.56	0.13	1.21	0.34	–

**Fig. 2.** The spectra of the $3 < z < 4$ quasars which were taken with grism 600 B. The flux is given in units of $[10^{-15} \text{ erg s}^{-1} \text{ cm}^{-2} \text{ \AA}^{-1}]$

and OVI1034/HeIII 640 to estimate the relative abundance of the line emitting gas. Comparison with Fig. 6 of Hamann & Ferland (1999) indicates that the measured line ratios provide a consis-

**Fig. 3.** Spectrum of SDSSpJ033829.31+002156.3. The flux is given in units of $[10^{-17} \text{ erg s}^{-1} \text{ cm}^{-2} \text{ \AA}^{-1}]$

tent range for the metallicity only for the rapid star formation model. The estimated line ratios for the four quasars with $z \approx 3$ are given in Table 4. Although the scatter of the measurements is large, a supersolar metallicity of $Z \approx 7 Z_{\odot}$ is indicated with an uncertainty of $\sim 5 Z_{\odot}$. This demonstrates that the metallicity of the line emitting gas of QSOs does not change significantly out to a redshift of $z \approx 5$. Assuming $\Omega_M=0.3$, $\Omega_{\Lambda}=0.7$ (for a flat universe – Carlberg et al. 1999; Perlmutter et al. 1999), and $H_0=65 \text{ km s}^{-1} \text{ Mpc}^{-1}$ such a redshift of $z = 5$ corresponds to an age of $\approx 1 \text{ Gyr}$ (Carroll, Press, & Turner 1992). Our NV/CIV and NV/HeII ratios fall into the range observed for other high-redshift quasars (Fig. 7 of Hamann & Ferland 1999) and fit well the “Giant Elliptical” nitrogen enrichment model of the quasar matter. Based on those evolutionary models the decrease of the relative nitrogen abundance expected for very high redshifts seems not to occur even to $z \approx 5$.

Two of the quasars in our sample (Q0046-282 and Q0338+0021) show broad absorption features (BALs) in their

Table 4. The derived relative abundance of the line emitting gas. The estimates based on the the rapid star formation model to describe the chemical enrichment of the gas.

object	NV/CIV	NV/HeII	OVI/HeII
Q0044-273	8.1	2.2	3.9
Q0046-282	17.5	7.1	15.5
Q0103-294	7.1	3.2	–
Q0103-260	10.3	3.7	14.5
Q0338+0021	13.0	4.6	–

spectra. In Q0046-282 the broad absorption are clearly visible at the CIV, Ly α , OVI1034, and Ly β lines. In the case of Q0338+0021 CIV1549 seems to have highly blueshifted BAL components with $v_{\text{blue}}^{\text{II}} \simeq -12000 \text{ km s}^{-1}$ and $v_{\text{blue}}^{\text{I}} \simeq -18000 \text{ km s}^{-1}$ (Fig. 3). The absorption feature I is also visible in the discovery spectrum of Fan et al. (1999) as well as the narrow absorption lines ($v_{\text{blue}}^{\text{II}}$). The strength of the strong CIV absorption ($v_{\text{blue}}^{\text{I}}$) in this object might indicate that the metallicity of the BAL gas is of the same order as for the BEL. Hence, both, BEL and BAL material, point towards supersolar abundances.

For Q0103-260 we found deep absorption features in the Ly α and CIV1549 emission line profile (Figs. 1,2). The velocity offset was measured to $v_{\text{abs}}^{\text{Ly}\alpha} \simeq 100 \text{ km s}^{-1}$ and $v_{\text{abs}}^{\text{CIV}} \simeq 760 \text{ km s}^{-1}$. Although both absorption lines show a similar width of FWHM $\simeq 1200 \text{ km s}^{-1}$ the velocity shift to the red is different.

At least two of the observed objects (Q0103-260 and Q0338+0021) show narrow metallic absorption lines in their spectra (Figs. 2,3). Moreover, Q0103-260 has a very rich Lyman forest spectrum. Hence, these two quasars are prime candidates for further studies with higher spectral resolution to derive the nature and physical properties of the intervening absorbing matter.

Acknowledgements. We would like to express sincere thanks to the staff of the Paranal observatory for the efficient and friendly support of the FORS commissioning team. We would also like to thank Michael Strauss and Xiaohui Fan (Princeton University Observatory) for providing the coordinates of SDSSpJ033829.31+002156.3 and useful comments for this letter. This work was supported by the German Science Foundation (Deutsche Forschungsgemeinschaft, projects SFB 328 and SFB 439) and by the German Federal Ministry for Education and Research (grants nos. 053HD50A, 053GO10A, and 053MU104).

References

- Carlberg, R.G., Yee, H.K.C., Morris, S.L., et al. 1999, ApJ, 516, 552
 Carroll, S.M. & Press, W.H. 1992, Ann.Rev.Astron.Astrophys., 30, 499
 Fan, X., Strauss, M.A., Schneider, D.P., Gunn, J.E., Lupton, R.H., et al. 1999, AJ, 118, 1
 Ferland, G.J., Baldwin, J.A., Korista, K.T., et al. 1996, ApJ, 461, 683
 Hamann, F. & Ferland G.J. 1992, ApJ, 391, L53
 Hamann, F. & Ferland, G.J. 1993, ApJ, 418, 11
 Hamann, F. & Ferland, G.J. 1999, Ann.Rev.Astron.Astrophys., 37, in press
 Korista, K.T., Hamann, F., Ferguson, J. & Ferland, G.J. 1996, ApJ, 461, 641
 Korista, K.T., Baldwin, J.A., Ferland, G.J., & Verner, D. 1997, ApJS, 108, 401
 Osmer, P.S., Porter, A.C., & Green, R.F. 1994, ApJ, 436, 678
 Perlmutter, S., Aldering, G., Goldhaber, G., et al. 1999, ApJ, 517, 565
 Pettini, M. 1999, in Proc of ESO Workshop on ‘Chemical Evolution from Zero to High Redshift’, eds. J. Walsh and M. Rosa, Springer, in press
 Schwarz, H.E. & Melnick, J. 1993, The ESO Users Manual, p.24